

Superconductivity and antiferromagnetism in $\text{Ba}_{0.75}\text{K}_{0.25}\text{Fe}_2\text{As}_2$ single crystals as seen by ^{57}Fe Mössbauer spectroscopy

J. Munevar,¹ H. Micklitz,¹ J. Agüero,¹ Guotai Tan,² Chenglin Zhang,^{2,3} Pengcheng Dai,³ and E. Baggio-Saitovitch^{1,*}

¹*Centro Brasileiro de Pesquisas Físicas, Rua Xavier Sigaud 150, Rio de Janeiro, Brazil*

²*Department of Physics and Astronomy, University of Tennessee, Knoxville, Tennessee 37996-1200, USA*

³*Department of Physics and Astronomy, Rice University, Houston, Texas 77005, USA*

(Received 11 October 2013; revised manuscript received 4 November 2013; published 25 November 2013)

We have performed detailed ^{57}Fe Mössbauer spectroscopy measurements on $\text{Ba}_{0.75}\text{K}_{0.25}\text{Fe}_2\text{As}_2$ single-crystal mosaics showing antiferromagnetic ordering below $T_N = 95$ K with superconductivity below T_C around 30 K. Analysis of the Mössbauer spectra shows a decrease in the magnetic hyperfine field but no change in the magnetic volume fraction below T_C . This indicates coexistence of magnetism and superconductivity in these compounds.

DOI: [10.1103/PhysRevB.88.184514](https://doi.org/10.1103/PhysRevB.88.184514)

PACS number(s): 74.70.Xa, 76.80.+y, 74.20.Mn

The coexistence of superconductivity (SC) and antiferromagnetism (AF) in the recently discovered iron-based pnictides is a heavily discussed subject.¹ Since it is the general opinion that both phenomena originate from Fe-3d electrons, a competition between these two phenomena may be expected. A decrease in the local magnetic field in muon spin rotation (μSR) recently has been observed in polycrystalline samples of $\text{Ba}_{1-x}\text{K}_x\text{Fe}_2\text{As}_2$.² It has been proposed that this result implies s^{+-} pairing of the Cooper pairs, meaning unconventional superconductivity and coexistence of SDW antiferromagnetism and superconductivity.³ However, such a decrease has not been observed for the muon precession frequency in Ni-doped BaFe_2As_2 .⁴ On the other hand, a decrease in the Bragg intensities for Ni- and Co-doped BaFe_2As_2 by neutron scattering measurements has been seen.^{5–10}

The Bragg intensities reflect the product of magnetic volume fraction and magnitude of magnetic moments, and the μSR and other local probe techniques measure the magnitude of local magnetic moments. These both results can be understood if there is a decrease in the magnetic volume fraction below T_C , but not a change in the magnitude of magnetic moments below T_C . The length scale of coexistence of the two phenomena, SC and AF order, appears to be another decisive parameter: phase separation on a mesoscopic length scale larger than the SC coherence length (about 2 nm¹¹), for example, has been proposed for $\text{Ba}_{1-x}\text{K}_x\text{Fe}_2\text{As}_2$.¹² In a recent paper, on the other hand, the coexistence of the two phenomena, SC and AF order, in $\text{Ba}_{1-x}\text{K}_x\text{Fe}_2\text{As}_2$ on a lattice parameter length scale has been claimed.¹³ The length scale of coexistence of the two phenomena, SC and AF order, in the above given iron-pnictides, therefore, is still an unsolved problem. In order to contribute to a better understanding of the above described open questions, we have performed detailed ^{57}Fe Mössbauer studies above and below T_C on single-crystal mosaics of $\text{Ba}_{0.75}\text{K}_{0.25}\text{Fe}_2\text{As}_2$ to see whether a change in the static Fe moment at T_C can be reflected in the local magnetic hyperfine field at the ^{57}Fe nucleus in this compound.

Single-crystal mosaics of $\text{Ba}_{0.75}\text{K}_{0.25}\text{Fe}_2\text{As}_2$ were used for Mössbauer studies, formed by thin platelets mounted in circled mosaics with roughly 1 cm of diameter. The details of crystal growth procedures are published elsewhere.¹⁴ Mosaics were mounted with c axis perpendicular to the absorber plane and parallel to 14.4 keV γ rays from the ^{57}Co source. Mössbauer

spectra were taken in a variable-temperature helium cryostat, allowing temperatures between 2 and 300 K. Both Mössbauer source ($^{57}\text{Co}:\text{Rh}$), moving in a sinusoidal mode, and absorber have been kept at the same temperature. Isomer shifts are given relative to that of $\alpha\text{-Fe}$.

The superconducting response of single crystals of $\text{Ba}_{0.75}\text{K}_{0.25}\text{Fe}_2\text{As}_2$ was measured in a SQUID magnetometer with an applied field of 30 Oe parallel to the ab plane, taking 2–45 K as temperature range. From this measurement (see Fig. 1) a diamagnetic response related to the onset of superconducting ordering is clearly observed in the zero-field-cooling mode. The superconducting transition temperature is around 33 K, while the superconducting volume fraction estimated from this measurement gives approximately 80%, indicating nearly full superconducting volume.

The ^{57}Fe Mössbauer spectra taken below T_N , i.e., in the magnetic regime, generally should be fitted within the SDW model with a distribution of magnetic hyperfine fields represented by a Fourier series expansion.¹⁵ However, as we have shown in another paper on ^{57}Fe Mössbauer spectroscopy in $\text{BaFe}_{2-x}\text{Ni}_x\text{As}_2$ pnictides, a “two-site model” can satisfactorily fit all spectra below T_N .⁴ In this “two-site model” a magnetic and a nonmagnetic site are used. Both sites have the same isomer shift and quadrupole splitting, i.e., correspond to the same crystallographic site. The nonmagnetic sites are related to nonmagnetic regions, probably caused by a distortion of the SDW magnetic structure due to doping. However, we should remark that using the simple “two-site model,” the nonmagnetic fraction that we obtain from such a fit will give us an upper limit for the nonmagnetic fraction. In the SDW model, part of the magnetic fraction will have very low magnetic field values and, therefore, the nonmagnetic fraction in the SDW model will be somewhat smaller. Despite the simplicity of our model, we will extract information on the interplay of SC and magnetism in this compound, which essentially is the goal of this work.

Mössbauer spectra in the temperature regime from 4.35 K to higher temperatures are shown in Fig. 2. From the spectra it is clearly observed that the resonance line begins to broaden below 90 K, caused by SDW order of the Fe moments in the ab plane. Above T_N , ^{57}Fe Mössbauer spectra shown in Fig. 2, exhibit a single line which has been fitted with an unresolved quadrupole doublet. The ^{57}Fe Mössbauer spectra

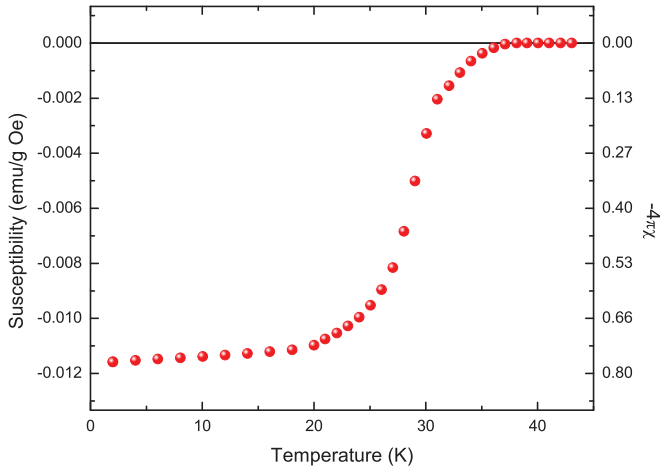


FIG. 1. (Color online) Magnetic susceptibility measurements performed on $\text{Ba}_{0.75}\text{K}_{0.25}\text{Fe}_2\text{As}_2$ single crystals, with 30 Oe applied field parallel to the ab plane.

taken below T_N have been fitted with a nonmagnetic and a magnetic components, having the same isomer shift and quadrupole interaction, and therefore corresponding to the same crystallographic site.

The nonmagnetic component was considered to be an unresolved quadrupole doublet similar to the one of the paramagnetic state, while the magnetic component was fitted

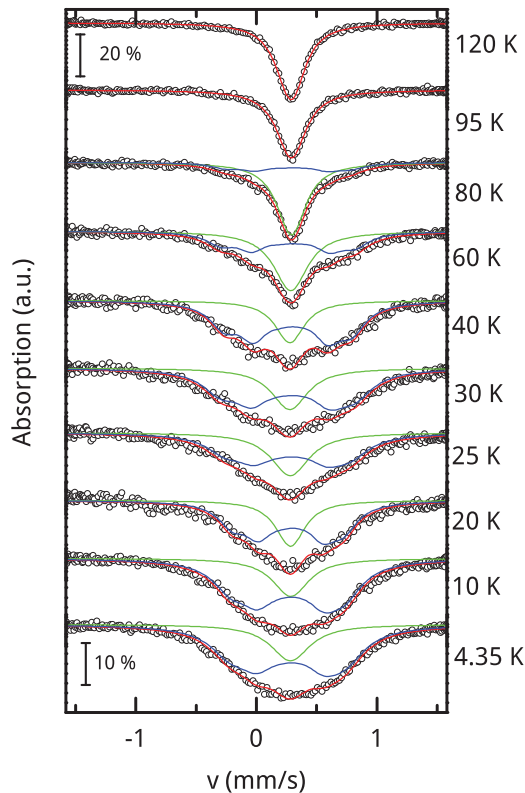


FIG. 2. (Color online) ^{57}Fe Mössbauer spectra for $\text{Ba}_{0.75}\text{K}_{0.25}\text{Fe}_2\text{As}_2$ single-crystal mosaics. γ ray is parallel to crystal c axis. Fits assuming a two-site model are shown, with a magnetic (blue lines) and a nonmagnetic (green single line) component below T_N .

within the full Hamiltonian model,¹⁶ essentially having seven fitting parameters such as magnetic hyperfine (hf) field, quadrupole interaction, angle between magnetic hf field and γ -ray direction (parallel to c axis), as well as that between main component V_{zz} of electric field gradient tensor and γ -ray direction, isomer shift, linewidth, and line intensity. The direction of V_{zz} is parallel to the c axis and B_{hf} is lying in the ab plane; i.e., the angle between V_{zz} and B_{hf} is 90° , while that between V_{zz} and the γ -ray direction is zero. We also fixed the linewidth to values obtained in the paramagnetic state.

From the fits described above, we can extract the isomer shift for both sites, the magnetic hyperfine field and the nonmagnetic volume fraction. The isomer shift was found to be $\delta = 0.38(1)$ mm/s, indicating that Fe is in +2 valence state. Quadrupole splittings are well known for their capability to reflect structural phase transitions affecting the Fe electric interactions. However, we did not find any indication of change in the quadrupole interaction at T_N , even knowing that a structural transition indeed exists. We have seen a change in the quadrupole splitting at T_N for the Ni-doped BaFe_2As_2 single crystals.⁴ This may indicate that K doping induces less disorder in FeAs tetrahedra rather than Ni doping at the Fe site. Linewidths never exceeded 0.4 mm/s.

Magnetic hyperfine field $B_{hf}(T)$, magnetic volume fraction, and weighted magnetic hyperfine (hf) field, defined as the product of the magnetic hyperfine field and the magnetic volume fraction, are shown for $\text{Ba}_{0.75}\text{K}_{0.25}\text{Fe}_2\text{As}_2$ in Fig. 3. Magnetic ordering is observed around 95 K showing a sharp increase of the magnetic moment for Fe. Nevertheless, the magnetic fraction of the sample starts to increase slowly below T_N , reaching a steady value only below 40 K. This also is observed with μSR for $\text{Ba}_{1-x}\text{K}_x\text{Fe}_2\text{As}_2$ polycrystalline samples² and in some other iron pnictides for the underdoped regime,¹⁷ and this may be caused by the doping influence on the local Fe structure. Below T_C (30 K) a decrease in B_{hf} is observed, in agreement with the μSR results on polycrystalline $\text{Ba}_{1-x}\text{K}_x\text{Fe}_2\text{As}_2$.² This important finding will be discussed in more detail below. The magnetic moment estimated from B_{hf} using the $6.3 \text{ T}/\mu_B$ relation found in Ref. 18 is around $0.48 \mu_B$, an indication of itinerant magnetism for Fe due to Fermi surface nesting.^{3,19,20} If we compare this value with that reported for BaFe_2As_2 ($\mu_{Fe} = 0.87 \mu_B$)¹⁸ we have to conclude that the decrease in the magnetic moment (or B_{hf}) is being induced by K doping on the Ba site, that is, by distortion of the Fermi surface resulting in a reduction of the nesting between hole and electron pockets. The weighted magnetic hf [Fig. 3(b)] field shows a temperature dependence of the Fe moment looking like an ordinary second-order phase transition. With a microscopic method (Mössbauer) we can distinguish between size of magnetic moment and magnetic volume fraction. With a macroscopic method (magnetization, neutron scattering) one only can measure the product of these 2 quantities. For that reason the magnetic phase transition looks like an ordinary second-order phase transition in neutron scattering experiments, while in our Mössbauer experiments it is more like a local first-order transition, triggered by the structural transition. It should be mentioned that the magnetic volume fraction does not reach 100% at low temperatures. This in principle is in contradiction with a previous work² where 100% magnetic volume fraction is reached below some temperature, but we

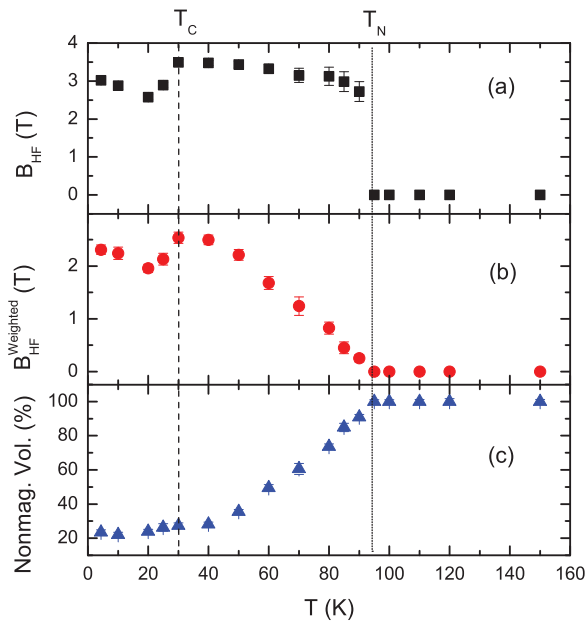


FIG. 3. (Color online) (a) Magnetic hyperfine field B_{hf} , (b) weighted B_{hf} , and (c) nonmagnetic volume fraction extracted from ^{57}Fe Mössbauer spectra fits for $\text{Ba}_{0.75}\text{K}_{0.25}\text{Fe}_2\text{As}_2$ single-crystal mosaics.

notice that this may be an indication of magnetic moments in $\text{Ba}_{0.75}\text{K}_{0.25}\text{Fe}_2\text{As}_2$ single crystals that can be sensed by μSR but not by Mössbauer spectroscopy, appearing in the latter as nonmagnetic sites in our simple two-site model (see above).

It is well known that in the iron pnictide systems the Fermi surface for the parent compounds is composed by two concentric electron pockets centered at (π, π) and two concentric hole pockets centered at $(0, 0)$ in the Brillouin zone. Nesting between electron and hole pockets gives rise to SDW order. Superconductivity occurs when nesting is weak, caused by distortion of the Fermi surface through doping or external pressure.¹⁹ When the system is doped with electrons, the electron pockets expand and the hole pockets contract, and the inverse happens when the system is hole doped.¹ This Fermi surface distortion reduces nesting and gives possibility to the appearance of Cooper interactions between electrons.²⁰ In the light of this information, we can think that for the case in which we have magnetic SDW ordering and superconductivity in the same sample, we can have phase separation with one of the phases still showing Fermi surface nesting and thus magnetic ordering, while for the other phase the Fermi surface nesting can be broken giving rise to superconductivity. On the other hand, we could also expect an overlap between magnetism and superconductivity, which means we would have at the same

time conditions to have Fermi surface nesting for weakened magnetism and favorable conditions to have Cooper pairing.

The data presented in Fig. 3 indicate that there is a connection between magnetic ordering and superconductivity: a decrease of the magnetic hyperfine field B_{hf} below T_C can be observed. Such a decrease only can be seen if we have either coexistence between magnetism and superconductivity or a phase separation on a length scale smaller than the superconducting coherence length ζ_{SC} . Since $\zeta_{SC} \sim 2$ nm,¹¹ which is of the order of the unit cell, it obviously does not make sense to talk about a real “phase separation.” Coexistence between magnetism and superconductivity, therefore, is indicated from our Mössbauer studies. Neutron scattering studies on the same samples^{5–8} show a decrease in the Bragg peak intensity accompanied by a resonance below T_C . This means that there is a decrease in the Fe magnetic moment or in the magnetic volume fraction, accompanied by a change in the Fe magnetic moment dynamics. Taking our Mössbauer results which clearly do not see a change in the magnetic volume fraction below T_C , but a decrease in the magnetic hyperfine field, we can conclude that there is a decrease in the Fe magnetic moment below T_C . It is argued that such a decrease is caused by a spectral weight transfer when entering the superconducting state. It can be explained by assuming s^{+-} pairing symmetry, where reentrance of the nonmagnetic phase occurs below T_C and thus reducing the Fe magnetic moment.³

In conclusion we can say that our ^{57}Fe Mössbauer studies indicate the coexistence of magnetism and superconductivity in single crystals of $\text{Ba}_{0.75}\text{K}_{0.25}\text{Fe}_2\text{As}_2$ which is seen as a reduction of the Fe magnetic moment below T_C . Our data are consistent with NMR measurements, which also show microscopic coexisting AF order and superconductivity.^{21–23} This clearly shows the advantages of using Mössbauer spectroscopy compared to other techniques, e.g., neutron scattering or μSR : (i) ^{57}Fe Mössbauer spectroscopy as a local technique can distinguish between the change of the local magnetic moment and that of the magnetic volume fraction, respectively; this, however, is not possible by neutron scattering; (ii) ^{57}Fe Mössbauer spectroscopy measures the magnetic moment directly at the probe (Fe) atom, while in μSR the site where the muon is coming to rest may be one or several sites away from the Fe position.

This work has been supported by the CNPq (under CIAM collaboration with NSF), CAPES, and the FAPERJ agency in Rio under several projects. The single-crystal growth efforts at UT/Rice were supported by the US DOE, BES, through Contract No. DE-FG02-05ER46202. H.M. acknowledges a visitor fellowship of CAPES and CNPq which supported work at CBPF.

*Author to whom correspondences should be addressed: elisa@cbpf.br

¹P. C. Dai, J. P. Hu, and E. Dagotto, *Nat. Phys.* **8**, 709 (2012).

²E. Wiesenmayer, H. Luetkens, G. Pascua, R. Khasanov, A. Amato, H. Potts, B. Banusch, H.-H. Klauss,

and D. Johrendt, *Phys. Rev. Lett.* **107**, 237001 (2011)

³R. M. Fernandes, D. K. Pratt, W. Tian, J. Zarestky, A. Kreyssig, S. Nandi, M. G. Kim, A. Thaler, N. Ni, P. C. Canfield, R. J. McQueeney, J. Schmalian, and A. I. Goldman, *Phys. Rev. B* **81**, 140501(R) (2010).

- ⁴C. Argüello *et al.* (unpublished).
- ⁵D. K. Pratt, W. Tian, A. Kreyssig, J. L. Zarestky, S. Nandi, N. Ni, S. L. Bud'ko, P. C. Canfield, A. I. Goodman, and R. J. McQueeney, *Phys. Rev. Lett.* **103**, 087001 (2009).
- ⁶A. D. Christianson, M. D. Lumsden, S. E. Nagler, G. J. MacDougall, M. A. McGuire, A. S. Sefat, R. Jin, B. C. Sales, and D. Mandrus, *Phys. Rev. Lett.* **103**, 087002 (2009).
- ⁷M. Wang, H. Luo, J. Zhao, C. Zhang, M. Wang, K. Marty, S. Chi, J. W. Lynn, A. Schneidewind, S. Li, and P. Dai, *Phys. Rev. B* **81**, 174524 (2010).
- ⁸M. Wang, H. Luo, M. Wang, S. Chi, J. A. Rodriguez-Rivera, D. Singh, S. Chang, J. W. Lynn, and P. Dai, *Phys. Rev. B* **83**, 094516 (2011).
- ⁹Huiqian Luo, Rui Zhang, Mark Laver, Zahra Yamani, Meng Wang, Xingye Lu, Miaoyin Wang, Yanchao Chen, Shiliang Li, Sung Chang, Jeffrey W. Lynn, and Pengcheng Dai, *Phys. Rev. Lett.* **108**, 247002 (2012).
- ¹⁰X. Lu, H. Gretarsson, R. Zhang, X. Liu, H. Luo, W. Tian, M. Laver, Z. Yamani, Y.-J. Kim, A. H. Nevidomskyy, Q. Si, and P. Dai, *Phys. Rev. Lett.* **110**, 257001 (2013).
- ¹¹M. Putti, I. Pallecchi, E. Bellingeri, M. R. Cimberle, M. Tropeano, C. Ferdeghini, A. Palenzona, C. Tarantini, A. Yamamoto, J. Jiang, J. Jaroszynski, F. Kametani, D. Abraimov, A. Polyanskii, J. D. Weiss, E. E. Hellstrom, A. Gurevich, D. C. Larbalestier, R. Jin, B. C. Sales, A. S. Sefat, M. A. McGuire, D. Mandrus, P. Cheng, Y. Jia, H. H. Wen, S. Lee, and C. B. Eom, *Supercond. Sci. Technol.* **23**, 034003 (2010).
- ¹²J. T. Park, D. S. Inosov, Ch. Niedermayer, G. L. Sun, D. Haug, N. B. Christensen, R. Dinnebier, A. V. Boris, A. J. Drew, L. Schulz, T. Shapoval, U. Wolff, V. Neu, X. Yang, C. T. Lin, B. Keimer, and V. Hinkov, *Phys. Rev. Lett.* **102**, 117006 (2009).
- ¹³W. K. Yeoh, B. Gault, X. Y. Cui, C. Zhu, M. P. Moody, L. Li, R. K. Zheng, W. X. Li, X. L. Wang, S. X. Dou, C. T. Lin, and S. P. Ringer, *Phys. Rev. Lett.* **106**, 247002 (2011).
- ¹⁴Y. Chen, X. Lu, M. Wang, H. Luo, and S. Li, *Supercond. Sci. Technol.* **24**, 065004 (2011).
- ¹⁵A. Olariu, P. Bonville, F. Rullier-Albenque, D. Colson, and A. Forget, *New J. Phys.* **14**, 053044 (2012).
- ¹⁶K. Ruebenbauer and T. Birchall, *Hyperfine Interact.* **7**, 125 (1979).
- ¹⁷A. J. Drew, Ch. Niedermayer, P. J. Baker, F. L. Pratt, S. J. Blundell, T. Lancaster, R. H. Liu, G. Wu, X. H. Chen, I. Watanabe, V. K. Malik, A. Dubroka, M. Rössle, K. W. Kim, C. Baines, and C. Bernhard, *Nat. Mater.* **8**, 310 (2009).
- ¹⁸P. Bonville, F. Rullier-Albenque, D. Colson, and A. Forget, *Europhys. Lett.* **89**, 67008 (2010).
- ¹⁹R. Chan, M. Gulacsi, A. Ormeci, and A. R. Bishop, *Phys. Rev. B* **82**, 132503 (2010).
- ²⁰Fa Wang and D. H. Lee, *Science* **332**, 200 (2011).
- ²¹G. F. Ji, J. S. Zhang, L. Ma, P. Fan, P. S. Wang, J. Dai, G. T. Tan, Y. Song, C. L. Zhang, P. Dai, B. Normand, and W. Yu, *Phys. Rev. Lett.* **111**, 107004 (2013).
- ²²S. Avci, O. Chmaissem, D. Y. Chung, S. Rosenkranz, E. A. Goremychkin, J. P. Castellán, I. S. Todorov, J. A. Schlueter, H. Claus, A. Daoud-Aladine, D. D. Khalyavin, M. G. Kanatzidis, and R. Osborn, *Phys. Rev. B* **85**, 184507 (2012).
- ²³Z. Li, R. Zhou, Y. Liu, D. L. Sun, J. Yang, C. T. Lin, and Guo-qing Zheng, *Phys. Rev. B* **86**, 180501 (2012).